Winter Monsoon Convection in the Vicinity of North Borneo. Part I: Structure and Time Variation of the Clouds and Precipitation

ROBERT A. HOUZE, JR.

Department of Atmospheric Sciences, University of Washington, Seattle 98195

SPIROS G. GEOTIS

Department of Meteorology, Massachusetts Institute of Technology, Cambridge 02139

FRANK D. MARKS, JR.

National Hurricane and Experimental Meteorology Laboratory, Coral Gables, FL 33146

ARTHUR K. WEST

Whatcom Community College, Bellingham, WA 98225

(Manuscript received 8 December 1980, in final form 20 April 1981)

ABSTRACT

Radar and satellite observations in the vicinity of northern Borneo obtained during the International Winter Monsoon Experiment (WMONEX) showed that the convection in that region underwent an extremely regular diurnal cycle. Over the sea to the north of Borneo, the general level of convective activity was increased during monsoon surges and during the passages of westward-propagating near-equatorial disturbances. Convective activity was decreased during monsoon lulls. The diurnal cycle was well-defined, regardless of whether the general level of convective activity was enhanced or suppressed by synoptic-scale events.

The cycle of convection over the sea was especially well documented. It was typically initiated at about midnight when an offshore low-level wind began. Where this wind met the monsoonal northeasterly flow, usually just off the coast, convective cells formed. After midnight, the convection continued to develop and by 0800 LST it had evolved into an organized mesoscale system with a precipitation area often continuous over a horizontal distance of 200 km. The structure of this system resembled that of squall lines and other organized mesoscale systems observed in the tropics. The precipitation was composed partially of convective cells, but a considerable portion was also stratiform with a well-defined melting layer extending across much of the system. This precipitation fell from a large mid-to-upper level cloud shield. The mesoscale systems typically began dissipating at midday, when the offshore wind reverted to an onshore wind and low-level convergence became concentrated over land.

1. Introduction

During winter, eastern Asia is dominated by a strong, steady monsoon, which develops as the continent cools and the Siberian anticyclone strengthens. At low levels, northwesterly flow occurs along the east coast of Asia at the latitude of Japan (Fig. 1a). Near the Tropic of Cancer (23°N), the flow turns southwestward and crosses the South China Sea toward the Indonesian-Malaysian complex of islands and peninsulas [called the "maritime continent" by Ramage (1968)]. Low-level convergence is concentrated in the vicinity of the cyclonic center located along the northern coast of the island of Borneo,[1] which lies in the center of the maritime continent. Rising motion and large amounts of rain occur over the maritime continent at this time. This region, moreover, is the location of the strongest upper level divergence in the global wintertime mean flow (Fig. 1b). The divergent component of the wind at 200 mb radiates outward from the maritime continent and feeds the Walker Circulation over the South Pacific, another tropical east-west circula-

[1] The entire island composed of the three nations East Malaysia (Sabah and Sarawak), Brunei and Indonesia (Borneo), is referred to in this paper by the single physical geographic name Borneo.

0027-0644/81/081595-20$09.00

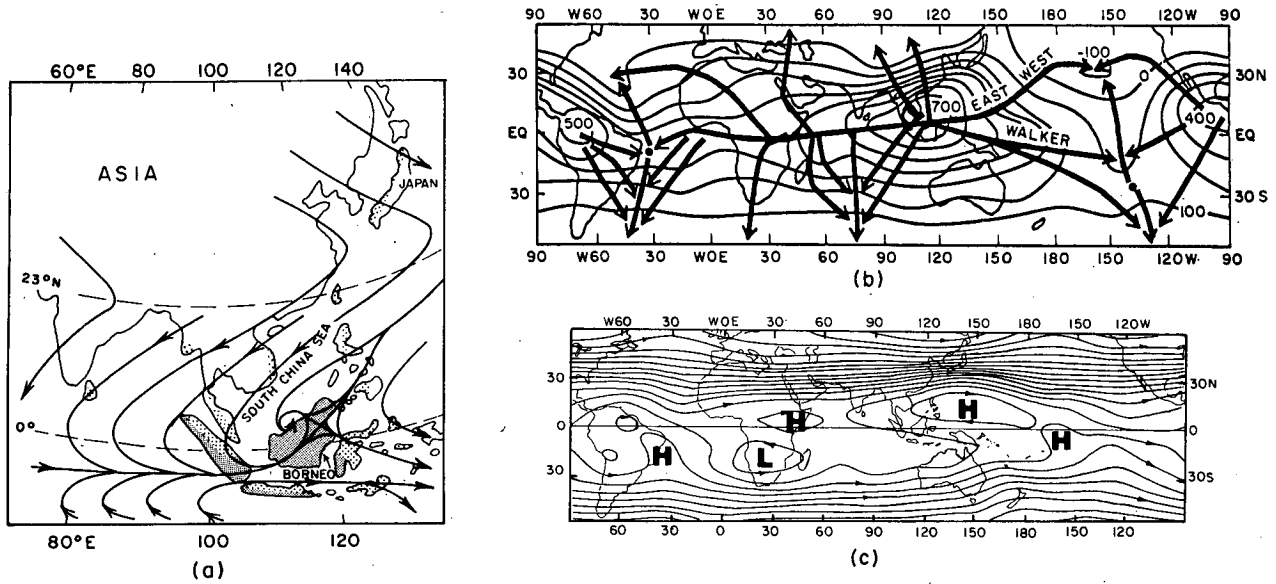

FIG. 1. Climatology of the Asian winter monsoon. (a) Gradient level winds and precipitation. Streamlines show wind direction. Black shading indicates 1 November–30 April rainfall over 152 cm. Gray shading indicates amounts from 76–152 cm. (b) Streamlines of the divergent part of the winter mean 200 mb wind shown with arrows. The arrows are orthogonal to isopleths of velocity potential χ (10^4 m^2 s^{-2}); contours are drawn for every 100 units. (c) Streamlines of the nondivergent part of the winter mean 200 mb wind shown by contours of streamfunction ψ (10^5 m^2 s^{-1}); contours drawn for every 50 units. Winds in (a) are from Atkinson and Sadler (1970); precipitation in (a) is from Cobb and Coleby (1966). Parts (b) and (c) are from Krishnamurti *et al.* (1973).

tion over the North Pacific, a similar circulation over the Indian Ocean, and the upper level return flow of the winter monsoon over eastern Asia (Krishnamurti *et al.*, 1973; Murakami and Unninayar, 1977). The return flow of the monsoon subsides in the Siberian anticyclone, north of the subtropical jet stream that passes over Japan (Blackmon *et al.*, 1977). This jet can be seen in the nondivergent component of the 200 mb level wind shown in Fig. 1c. It lies on the north side of the western Pacific upper level anticyclone. Borneo lies on the southwestern corner of this anticyclone, where the 200 mb flow is from the east-southeast.

Latent heat released in the clouds and precipitation that form in this region in winter constitutes one of the primary sources of energy for the atmosphere (Ramage, 1968). The importance of clouds over the maritime continent to the winter monsoon circulation is indicated by the results of numerical models. Using a two-level primitive equation model, Webster (1972) showed that by prescribing this heating as external forcing, along with similar but weaker prescribed heat sources over Africa and South America, the time-invariant general circulation of the entire tropics and subtropics can be simulated with considerable realism.

The importance of clouds in the winter monsoon is further indicated by examining the processes that maintain the eddy kinetic energy of the tropics during the Northern Hemisphere winter. This eddy kinetic energy is dominated by the longitudinal irregularity introduced into the wind fields of low-latitudes by the Asian winter monsoon over the maritime continent and similar planetary-scale eddies over Africa and South America. This kinetic energy is maintained by two processes—eddy pressure interaction with higher latitude circulations (i.e., the convergence of the flux of energy from higher latitudes associated with the correlation of wind and pressure fluctuations) and the baroclinic conversion of eddy available potential energy to eddy kinetic energy associated with the coincidence of large-scale rising motion and higher temperatures over the equatorial and maritime-continental heat sources. Using a multilevel general circulation model, Manabe *et al.* (1970) showed that in the upper troposphere the planetary-scale circulations of the tropics in winter can be maintained qualitatively correctly in a dry model by the pressure interaction effect alone. However, no planetary-scale eddy kinetic energy occurs in the lower troposphere of the dry model. When the effects of clouds are added to the model, through adjustment of the lapse rate for moist convection, vertical coupling between the lower and upper troposphere is established, and planetary-scale monsoonal circulations extend throughout the depth of the troposphere in a realistic fashion.

Thus, it is evident that the clouds and precipitation over the maritime continent and the vertical motions associated with them are essential to the winter monsoon as sources and sinks of condensational heating and as mechanisms for distributing the released heat vertically through the troposphere. Moreover, from studies such as those of Gray and Jacobson (1977) and Webster and Stephens (1980), it is apparent that the cloud cover significantly affects the vertical distribution of radiative heating in the vicinity of the maritime continent.

The structure of monsoon clouds has been described previously only in the broadest terms. Ramage (1971) categorized monsoon precipitation into "showers" from towering cumulus and cumulonimbus and "rains" from deep nimbostratus with embedded cumulonimbus. The observation of the latter type of precipitation indicates that both stratiform and convective air motions can occur in association with monsoon clouds and that the precipitation may be widespread as well as localized.

It also has been noted that the clouds and precipitation of the winter monsoon are sensitive to both synoptic-scale fluctuations and subsynoptic-scale variations of the planetary-scale monsoonal flow in the vicinity of the maritime continent. For example, heavy rainfalls on the north coast of Borneo are associated with "cold surges," during which a general strengthening of the low-level winds over the South China Sea occurs nearly simultaneously with a cold frontal passage at Hong Kong (Ramage, 1971). On other occasions, heavy precipitation over Borneo accompanies the passage of westward propagating disturbances, or waves, moving across the South China Sea from the equatorial Pacific Ocean (Cheang, 1977; Chang *et al.*, 1979). On the subsynoptic scale, land-sea contrasts, orography and the diurnal cycle in radiative heating combine to drive local circulations, which influence the rainfall over and near the various islands and peninsulas (Ramage, 1971; Short and Wallace, 1980).

One of the major goals of the International Winter Monsoon Experiment (WMONEX) was a better description and understanding of winter monsoon clouds and precipitation, both in terms of their structure and their relationship to large-scale and local flow patterns.

In this study, we make use of special observations obtained during December 1978, the intensive observation period of WMONEX, to examine winter monsoon clouds and precipitation. The primary data are radar observations obtained over northern Borneo and the adjoining southern South China Sea. Borneo lies in the center of the maritime continent and is the focus of the upward branch of the planetary-scale monsoon. Some 300–500 mm of rainfall along the northern coast of Borneo during a typical December, and in WMONEX a substantial number of the convective systems responsible for this typical rain were sampled by radar.

By describing the WMONEX convective systems in sufficient detail, we expect to elucidate two aspects of the monsoonal atmosphere's convective response to larger scale forcing. First, the time variation of the convective response will be shown by determining the extent to which the convection was modulated on diurnal and synoptic time scales. Second, the nature of the cloud-scale vertical motions, which, as noted above, link the the lower and upper level components of the planetary-scale monsoon, will be investigated by examining the relative degrees to which the clouds and precipitation exhibited convective or stratiform structure. In a companion paper by Johnson and Priegnitz (1981), similar objectives are pursued with rawinsonde data from the WMONEX ship array just north and west of the area of radar observations. The observed convective systems tended to form in the radar area and drift west-northwestward into the ship network. Consequently, a fuller understanding of the convection emerges from the two studies together than from either one alone.

2. Data

a. Radar observations

During WMONEX, the Massachusetts Institute of Technology's WR73 C-band weather radar was installed on the north coast of Borneo at Bintulu, Sarawak, East Malaysia, where it was operated without significant interruption from 8 to 31 December 1978. The characteristics of the radar system are summarized in Table 1. The same radar system was used in the Global Atmospheric Research Programme's Atlantic Tropical Experiment (GATE) on the Research Vessel *Gilliss*. It is equipped with a computer that controls the automatic operation of the radar, processes the returned signals, and records the data. In WMONEX, data were taken by repeatedly running the antenna through a prescribed sequence of conical scans. From this sequence, which took ~8 min to complete, three-dimensional echo structure can be determined. A sequence was initiated once every 10 min throughout the experiment.

b. Satellite imagery

Meteorological satellite observations were obtained during WMONEX with the Japanese geosynchronous satellite. In this study, we have used microfilm images of the infrared photography obtained at 0000, 0300, 0600, 0900, 1200, 1600, 1800

TABLE 1. MIT WR73 radar characteristics.

Wavelength	5.30 cm
Pulse length	300 m
PRF	250 s^{-1}
Peak power	250 kW
Beam width	1.45°
Azimuth averaging interval	1.0°
Azimuth recording interval	1.0°
Range bin size	0.25–1.0 km
Maximum range recorded	256 km

and 2100 GMT.[2] For years prior to Winter MONEX, we have used twice daily (0900 and 2100 LST) infrared images on microfilm from polar orbiting U.S. satellites.[3]

c. Synoptic data

Surface and pilot-balloon data from stations in northern Borneo were obtained from the Malaysian Meteorological Service.

3. Organization of the analysis around the diurnal cycle

That the clouds and precipitation over Borneo and its surrounding waters have a strong diurnal modulation was recognized *a priori*, both from studies of past data (Ramage, 1971; Short and Wallace, 1980) and from our monitoring of the WMONEX radar and satellite data while it was being taken. Consequently, we organized our analysis around the diurnal cycle. In the following sections, we consider (i) how well the diurnal cycle of convective response was maintained throughout the experiment; (ii) the relationship of the diurnal cycle of cloud and precipitation development to the diurnal land-sea wind oscillation associated with Borneo; (iii) the sensitivity of the diurnal convective cycle to intermittent synoptic-scale influences; and (iv) the convective versus stratiform structure of the diurnally generated clouds and precipitation.

4. Horizontal distributions of cloud and precipitation at various times of day

Short and Wallace (1980) used infrared radiance data in digital form from 0900 and 2100 LST satellite observations for the summer of 1975 and winter of 1976 in a global analysis of diurnal variations in cloud cover. Their winter season results show that the cloud cover in the vicinity of Borneo was dominated by high cloud tops generated by deep convection, with the cloudiness over land being much greater at 2100 LST than 0900 LST, while in a region a few hundred kilometers wide surrounding the island the cloudiness over water was much greater at 0900 LST than at 2100 LST. This behavior typifies large tropical islands, and Short and Wallace attribute the result to the generally held view that the convection over and near such islands is modulated by the diurnal variation of the boundary-layer circulation, which favors afternoon and evening cloudiness over the islands and later night and morning cloudiness over coastal waters.

Examining the northern portion of Borneo and the immediately surrounding southern South China Sea in more detail, we analyzed photographic images of the 0900 and 2100 (all times LST) infrared satellite data for three Decembers (1974, 1976 and 1977). Areas of high (cirriform) cloud tops were identified visually in a manner similar to studies such as those of Payne and McGarry (1977) and McGarry and Reed (1978). Contour patterns of the fractional area covered by high cloud are shown in Fig. 2. Subtraction of the 2100 pattern from that at 0900 results in contours qualitatively very similar to Short and Wallace's (1980) pattern of winter season differences between 0900 and 2100 outgoing IR radiance in the vicinity of Borneo. Consequently, we are confident that our visual method leads to results consistent with the numerical satellite data.

The major feature of the 0900 cloud cover patterns is a maximum centered offshore north-northwest of Bintulu (Fig. 2a). As will be shown below, this feature is associated with convection that forms offshore near midnight in response to the land breeze. Concentration of the nocturnally generated cloudiness in the region of the maximum is probably associated with the concave coastline and the concave mountain range inland, which at night must tend to focus [in the manner suggested by Neumann (1951)] both the land-sea and mountain-drainage winds in the region just offshore from Bintulu. At 2100 LST, the maximum of high cloud cover is centered over land several hundred kilometers south of Bintulu (Fig. 2b).

The cloud-cover pattern during December 1978 (Fig. 3), the period of WMONEX, was determined from the Japanese geosynchronous satellite data and found to be similar to the 3-year December climatology shown in Fig. 2. The morning maximum of cloudiness offshore was again prominent, but displaced some 200 km south of its 3-year average position (cf. Figs. 2a and 3a). The evening maximum over land south-southwest of Bintulu was in about the same position as in the 3-year average (cf. Figs. 2b and 3c).

Since the Japanese satellite was geosynchronous,

[2] Data obtained from Japan Weather Association, Kaiji Center Bldg. 5, 4-Chome, Kojimachi Chiyoda-Ku, Tokyo 102.

[3] Data obtained from the National Climatic Center, Asheville, North Carolina 28801.

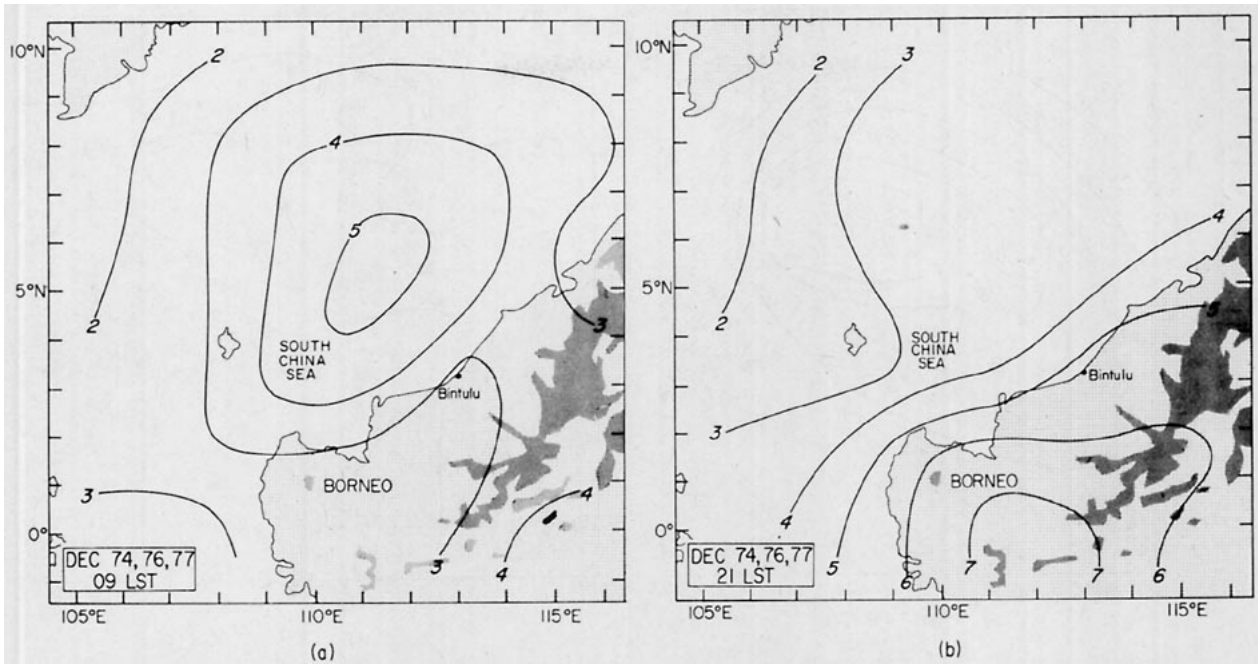

FIG. 2. Mean December patterns of the fractional area covered by upper level cloud at 0900 and 2100 LST, determined from infrared satellite data for three years. Contours are labeled in tenths and were drawn for data in 220 km × 220 km grid squares. Shading within Borneo shows land areas above 3000 ft (914 m) altitude.

patterns for times intermediate between morning and evening could be derived (Figs. 3b and 3c). From Figs. 3a and 3b, it can be seen that between 0800 and 1400 the maximum in morning cloudiness offshore drifted west-northwestward. This motion is in the direction of the typical 200–300 mb mean flow in this region in December (Fig. 1c). This steering level would be expected for an upper tropospheric cloud generated by earlier convection. After 1400, the offshore cloudiness dissipated, convection formed over land, and by 2000 (Fig. 3c) the maximum cloud cover over land south-southwest of Bintulu was established. At 0200 (Fig. 3d), the broad maximum extending from Bintulu south-southwestward was a transitional feature composed of the remains of the afternoon-generated convection far to the south-southwest and nocturnally generated convection just becoming established along the coast near Bintulu. After 0200, the clouds over land disappeared, while nocturnally generated convection expanded, moved farther offshore and became the early morning maximum seen offshore at 0800.

The horizontal distribution of fractional area covered by radar echo (i.e., precipitation) detected by the Bintulu radar is shown by hour of the day in Fig. 4. To obtain these patterns, the fractional area covered by echo on the 1.5° elevation angle radar scan was determined visually in 40 km × 40 km grid squares over the entire radar pattern. Patterns for a given hour of the day were averaged over all the days on which data were obtained between 8 and 31 December 1978.

The patterns thus derived are quite consistent with the diurnal cycle seen in the satellite data (Figs. 2 and 3). The maximum average echo coverage at 2000 was over land (Fig. 4a). It was probably actually centered south-southwest of the radar in a position similar to that of the maximum upper-level cloudiness detected by satellite (Fig. 3c). However, this region was blocked to the radar at low elevation angles by nearby buildings. By 0000, the precipitation over land typically was diminishing, while new echoes were forming just offshore (Fig. 4b). The precipitation over land had usually disappeared by 0400, while the offshore rain area had increased in size (Fig. 4c). From 0400–1600, the offshore echo region generally moved west-northwestward, reaching its maximum size at about 0800 (Figs. 4c–4f). This west-northwestward motion of the precipitation area agrees with the movement of the area of maximum upper level cloud cover seen offshore between 0800 and 1400 (Figs. 3a and 3b). As the offshore feature weakened, the onshore echo activity became established again. Consequently, the offshore echo was usually almost gone by 1600, while from 1600–2000 the onshore precipitation continued to intensify.

5. Mean diurnal cycles of cloud and precipitation coverage offshore and over land

The diurnal variations of the cloud and precipitation patterns observed by satellite and radar,

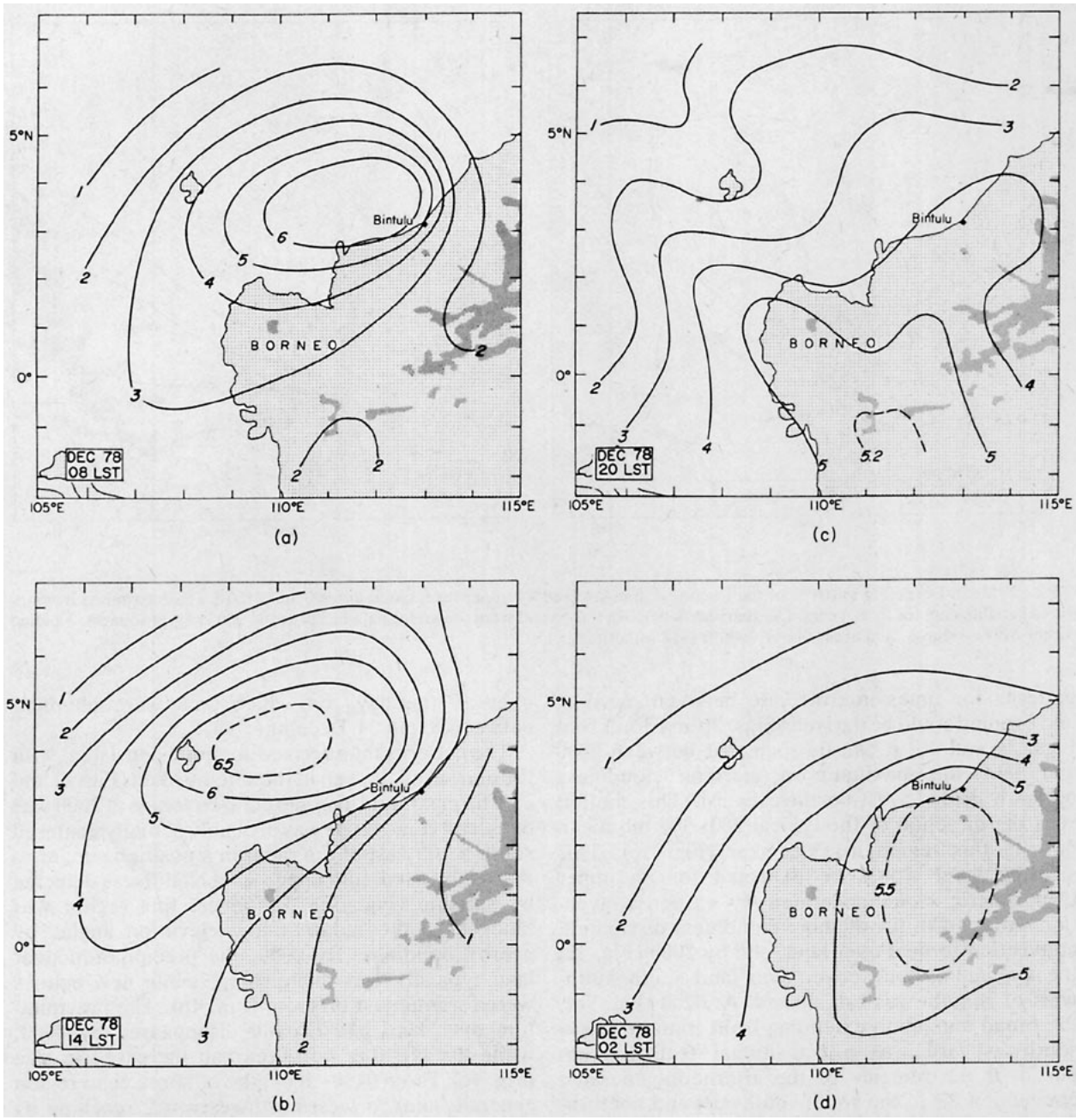

FIG. 3. Mean patterns of the fractional area covered by upper level cloud for various times of day, determined from infrared satellite data for December 1978. Contours are labeled in tenths and were drawn for data in 275 km × 275 km grid squares. Topographical contours as in Fig. 1.

respectively, can be further seen by dividing them into sea and land components. The regions designated sea and land for satellite observations are shown in Fig. 5. The sea and land regions for radar were obtained by dividing the area of radar coverage, shown in Fig. 4, along an azimuthal line extending northeastward from the radar site. The fractional areas covered by cloud or echo in sea and land regions are shown as functions of time in Figs. 6 and 7, respectively. The satellite cloudiness curves (Fig. 6) were derived from the same manually tabulated, visual estimates of the high-cloud coverage used to construct Fig. 3. Consequently, the resolution in time is only 6 h. The curves shown in the figure are fourth-order polynomials forced to fit five points. These objectively determined curves allow the times

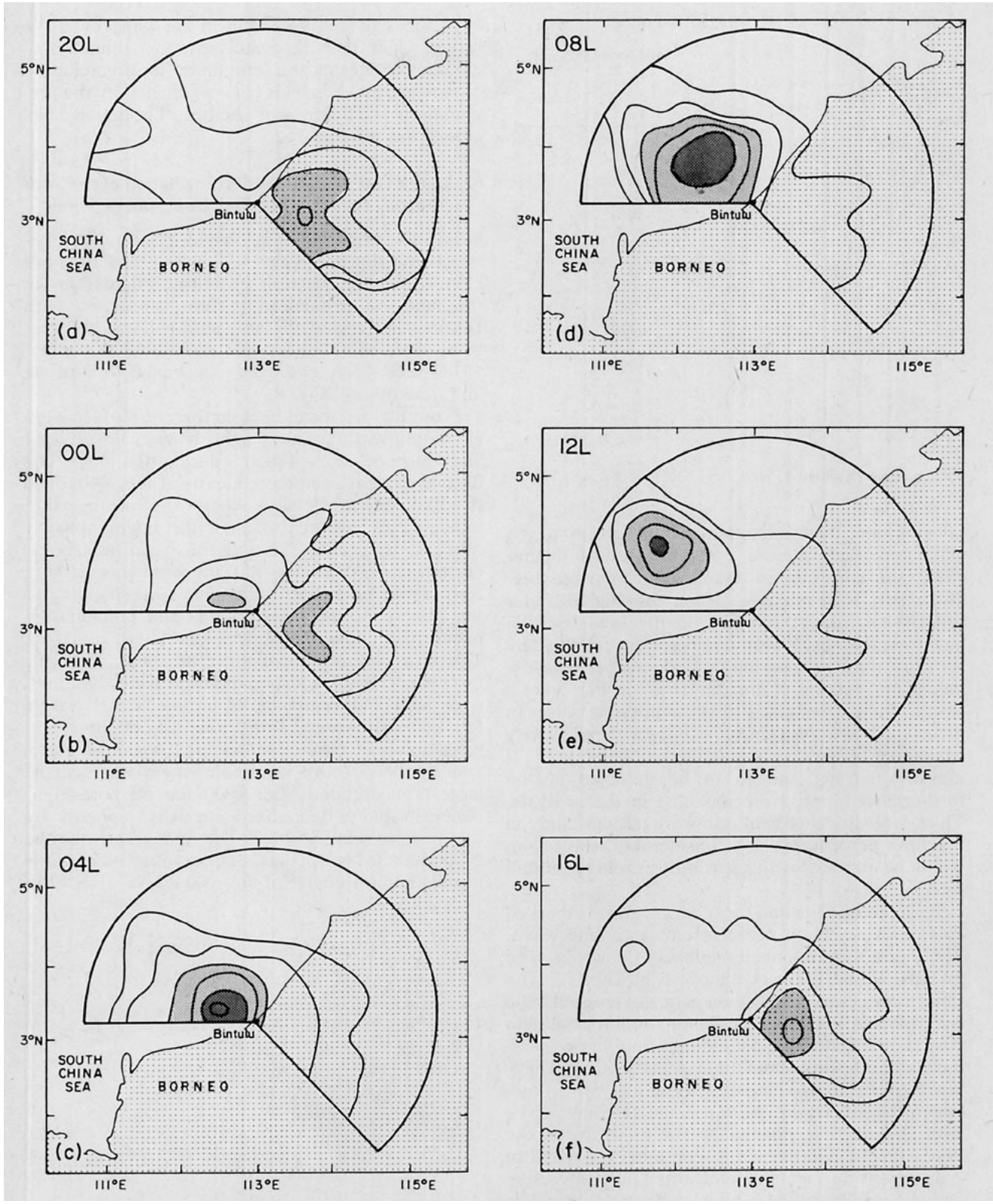

FIG. 4. Mean patterns of the fractional area covered by precipitation detected by the MIT radar at Bintulu for various times of day, averaged over the period 8–31 December 1978. Contours are for fractional area coverages of 0.1, 0.2, 0.3, 0.4, 0.5 and 0.6. The outer contour is for 0.1, the intermediate shading begins at 0.3 and the heavy shading at 0.5. The contours were drawn for data in 40 km × 40 km grid squares.

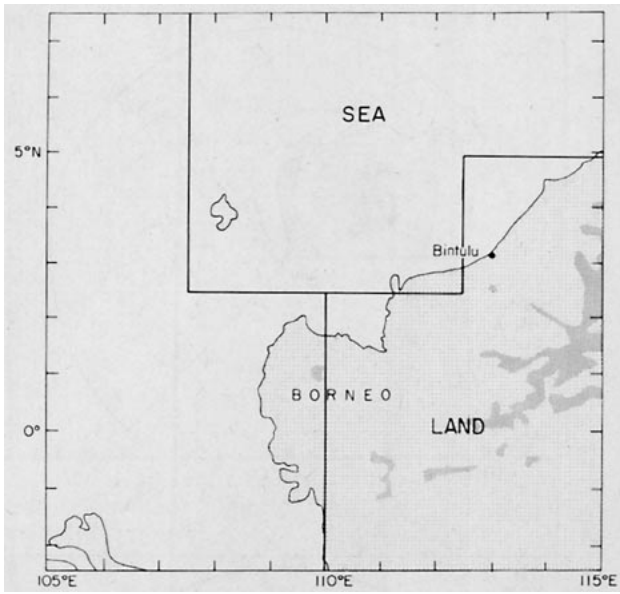

FIG. 5. Areas designated "land" and "sea" in obtaining Fig. 6.

of minimum and maximum cloud cover to be estimated. The diurnal cycle is seen in higher resolution in the curves of radar echo coverage (Fig. 7), which were derived from the digital radar reflectivity values recorded on the low-elevation angle scans for each hour that data were collected by the radar during the period 8–31 December. The low values of "percent of area covered" in Fig. 7 are a result of measures taken to avoid possible biases in the analysis procedure. Only echoes with reflectivity exceeding 27 dBZ (corresponding to a rain rate of ~2 mm h^{-1}), strong enough to be detected at the furthermost range, were included in the analysis. Thus, large areas of light rain were left out, and the resulting percentages are considerably lower than would be obtained with a lower threshold of rainfall rate.

Both the satellite and radar curves show a marked diurnal cycle. Each curve resembles a sine wave. The times of maxima and minima of the waves seen in Figs. 6 and 7 are summarized in Table 2. The radar curves show maximum echo coverage at 0800 over the sea and 2300 over land, while the satellite curves (estimated by polynomial fits) show maximum cloudiness at about noon over the sea and midnight over land. The substantial lag (~4 h) between the maxima of the radar and satellite curves over the sea is explained by the tendency of the upper level cloud shields to continue to expand in a divergent flow pattern aloft after the convective and mesoscale vertical motions that were responsible for producing the precipitation began to weaken. A similar lag occurred in the maxima over land but was not as great (only about an hour). The difference in the lagtimes in maxima (1 h over land 4 h over the sea) could be due to sampling or curve fitting. Over both land and sea, the minimum of cloudiness lagged the minimum in precipitation coverage by 4–5 h. This lag is explained by the precipitation declining well before the upper level cloudiness disappeared.

6. Association of cloud and precipitation cycles with diurnal variation of lower tropospheric winds

To investigate the probable relationship between the diurnal cycles of onshore and offshore clouds and precipitation to diurnal fluctuations in the land-sea circulation pattern associated with Borneo, surface winds and pilot-balloon observations from Bintulu for the period of December 1978 have been averaged according to altitude and time of day (Fig. 8).

From Fig. 8a, it can be seen that the surface wind at Bintulu was extremely light. It was calm at night and onshore at 3–4 m s^{-1} during the day. The diurnal cycle is seen more clearly at the 1000–5000 ft (305–1524 m) levels, where the mean wind, indicated by the centroids of the hodographs, is north-easterly at 3–7 m s^{-1}, the basic monsoonal current. At 1000 ft (Fig. 8b), the wind was onshore from about noon until midnight, corresponding to the period during which clouds and precipitation occurred predominantly over land (Figs. 6 and 7). The flow changed to offshore at about midnight, just when clouds and precipitation were dying out over land and beginning over the coastal waters (cf. Fig. 4b). Around 0800, when the offshore precipitation was most extensive (cf. Figs. 3a, 4d, 6 and 7), the offshore wind component was near its largest magnitude. After 0800 the offshore component rapidly decreased and was replaced by the onshore wind at 1400. The hodographs for the 2000–5000 ft levels (Figs. 8c–8e) followed patterns rather similar to those at the 1000 ft level (Fig. 8b).

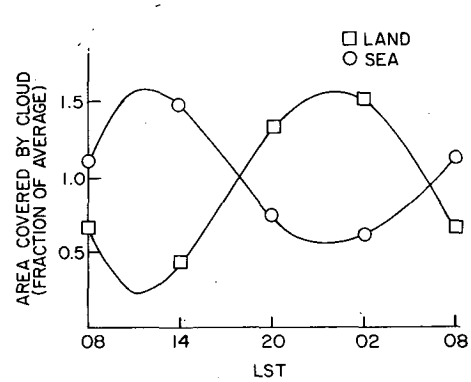

FIG. 6. Diurnal cycles of the fractional area covered by upper level cloud, seen in infrared satellite imagery within the "land" and "sea" areas located in Fig. 5, and averaged over the month of December 1978. The smooth curves are fourth-order polynomials fitted to five points.

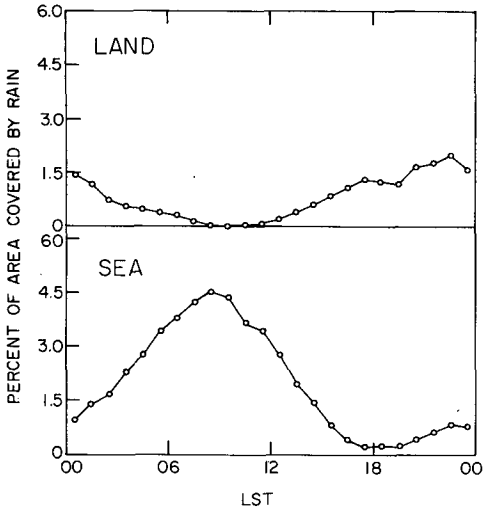

FIG. 7. Diurnal cycles of the fractional area covered by precipitation, observed over land and sea by the MIT radar at Bintulu, and averaged over the period 8–31 December 1978.

From these wind data and the foregoing discussions of the diurnal cycles of cloudiness and precipitation over land and sea, it is evident that a strong diurnal cycle of land-sea circulation associated with the island was superposed on the northeasterly monsoon current at low levels and that the net diurnal variation of the wind, in turn, controlled the atmosphere's convective response near North Borneo. Specifically, when the offshore wind component (generated diurnally) begins near midnight, there results an immediate commencement of convection over the sea. The large-scale convergence is then locally concentrated where the diurnal land breeze meets the low-level monsoon flow. The area covered by precipitation over the sea continues to build up after this time for as long as the land breeze prevails. At about midday, when the land breeze abruptly ends and the sea breeze begins, the region of most intense convergence shifts inland.

7. Regularity of the diurnal cycle during December

That the diurnal variation of cloud and radar echo coverage was a persistent phenomenon, observed each day during the experiment, and not just the result of a few days of strong diurnal variability averaged with many days of little or no diurnal variation, is shown by plotting the areal coverage over land and sea as functions of time (Figs. 9 and 10). From these plots, it is evident that the offshore feature reached a maximum area once every day from 8–31 December and reached a minimum at a time roughly midway between each maximum. The cycle over land was equally reliable, though it appears more clearly in the curve for satellite cloud cover (Fig. 9) than for the radar echo coverage (Fig. 10), probably because the diurnally generated convection over land was most concentrated well to the south-southwest of the region of radar observations (cf. Fig. 3c), whereas the offshore convection was centered well within radar range (cf. Fig. 3a).

8. Influence of synoptic-scale conditions on the convective response

In addition to the pronounced diurnal cycles of convection controlled by Borneo's diurnal modulation of the low-level northeasterly monsoonal flow, there were periods of 1–5 days duration in which the general level of cloudiness and precipitation, on which the diurnal cycle was superimposed, was alternately increased or subdued (see smoothed curves in Figs. 9 and 10). To determine whether these periods were associated with synoptic-scale fluctuations of the winter monsoon flow, we refer to Figs. 2 and 6 of the companion paper by Johnson and Priegnitz (1981). In their Fig. 2, monsoon surges are indicated by peaks in the average wind speed ($\bar{V}$) over the southern South China Sea along 7°N. The periods of surges ($\bar{V} > 10$ m s^{-1}) are indicated by the letter S in our Figs. 9 and 10. Lulls or minima in the wind speed record ($\bar{V} < 7$ m s^{-1}) are indicated by L. Johnson and Priegnitz' Fig. 6 indicates the westward progression of low-latitude disturbances, or easterly waves. The times that the centers of these disturbances crossed longitude 113°E (the meridian of Bintulu) are indicated by W in our Figs. 9 and 10.

From Fig. 9a, it is evident that the general level of cloudiness over the sea was increased during the periods of surges and decreased during lulls in the northeasterlies. The wave disturbance on 23 December may have also influenced the increase of cloudiness on that day. The disturbance reaching 113°E on 20 December was dying (dashed line in Johnson and Priegnitz' Fig. 6) and probably too weak to have much effect at that time. The lull was the dominant synoptic feature on that day. These results are consistent with earlier studies

TABLE 2. Times (LST) of maximum and minimum areal coverage by precipitation observed by radar (R) and clouds observed by satellite (S) over areas designated sea and land.

	Maximum	Minimum
Sea		
R	0800	1900
S	1200	0000
Land		
R	2300	0800
S	0000	1200

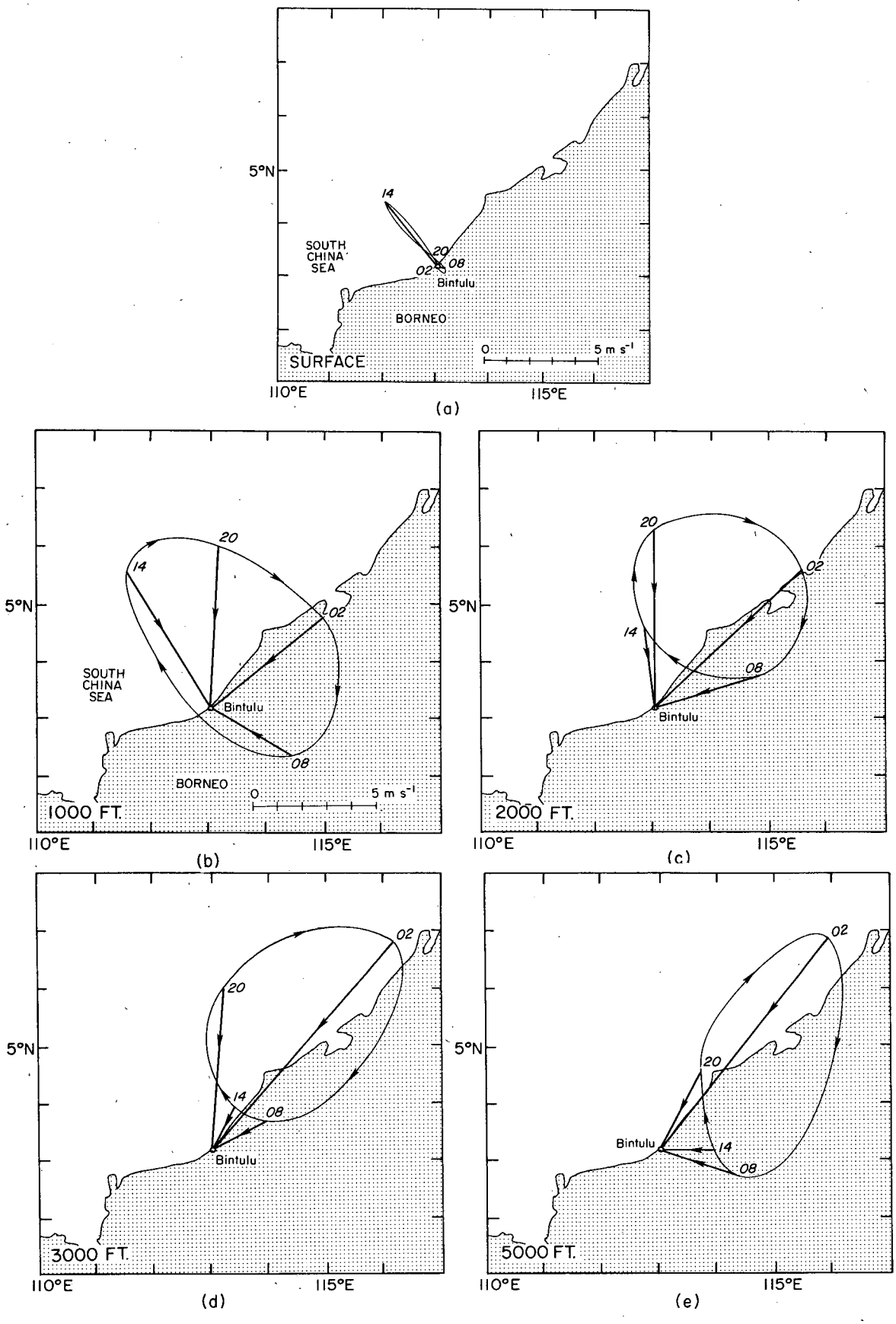
5°N
14
20
02
08
Bintulu
SOUTH CHINA SEA
BORNEO
SURFACE
0 5 m s⁻¹
110°E
115°E
(a)
1000 FT.
(b)
2000 FT.
(c)
3000 FT.
(d)
5000 FT.
(e)

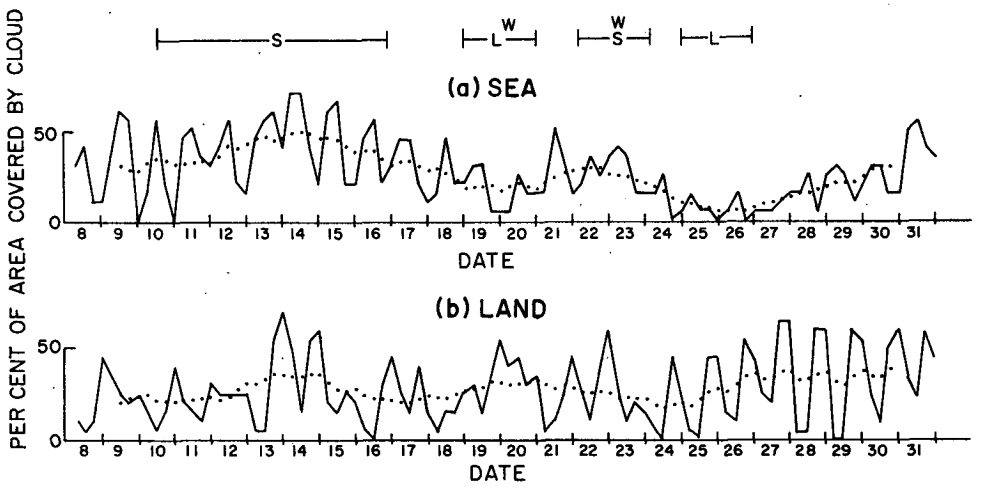

FIG. 9. Time-series of percent of area covered by upper level cloud, seen in infrared satellite imagery within the "land" and "sea" areas located in Fig. 5. Solid curves show unfiltered observations at 6 h intervals. Dotted curves show overlapping 60 h means. S, W and L denote periods of surges, waves and lulls in the synoptic-scale winds. Tick marks are at 0000 LST.

indicating that surges and disturbances increase convective activity along the northern Borneo coast and the adjacent southern South China Sea (Ramage, 1971; Cheang, 1977; Chang *et al.*, 1979). The general level of cloudiness over Borneo itself ("land", Fig. 9b) showed little or no correlation with the synoptic-scale events over the South China Sea. Thus, it was primarily the offshore convective activity, north of the island, that appeared to be sensitive to synoptic-scale fluctuations of the northeasterly flow over the sea.

The synoptic-scale variations in offshore convective activity were not as strongly apparent in the time series of radar echo coverage (see heavy curve in Fig. 10a) as in the time series of satellite cloudiness (smoothed curve in Fig. 9a). However, the general trends of the two curves are similar except around 10 December. This difference can be understood by noting that the satellite curve was derived for an area large enough that its net cloudiness should have generally reflected changes in synoptic-scale conditions (Fig. 6). The area represented by the offshore radar curve on the other hand was much smaller and located in the region where local diurnally generated convection was most favored (cf. Figs. 4d and 5). On the morning of 10 December, the local diurnal modulation of convection produced a particularly strong feature, and the radar echo over the sea showed a large peak (Fig. 10). However, the clouds and precipitation that occurred were localized to the offshore area near the radar. Elsewhere over the larger area covered by satellite, cloudiness was rather slight (see Fig. 7 of Johnson and Priegnitz, 1981). Consequently, the synoptic-scale trend in satellite cloudiness showed a minimum at this time (dotted curve, Fig. 9a). Evidently, the smaller area covered by radar was not representative of larger, synoptic-scale conditions on this day.

As in the case of the satellite data, the general trend in the amount of area covered by radar echo over land (smooth curve in Fig. 10b) showed no obvious relationship to the synoptic situation over the South China Sea. The amount of echo remained at about the same level throughout the experiment.

9. Life cycle and structure of the diurnally generated offshore cloud region

Since the precipitation over the sea, which reached its peak activity in the morning, was so well sampled by radar (Fig. 4d), its development and structure could be studied in detail. In this section, we examine four cases that typify its behavior. These cases are for 10, 16, 18 and 23 December 1978. From Fig. 10a, it can be seen that the precipitation over the sea was well developed on all four of these days. The four examples were chosen both because they were well defined and because they were centered close to the shore, where the vertical resolution of the radar scans was optimal.

The evolution of the four offshore areas is sum-

FIG. 8. Hodographs of winds observed at 0200, 0800, 1400 and 2000 LST by pilot balloon tracking at Bintulu and averaged over December 1978. Vectors indicate direction from which wind is blowing toward Bintulu. Note 1000 ft = 305 m.

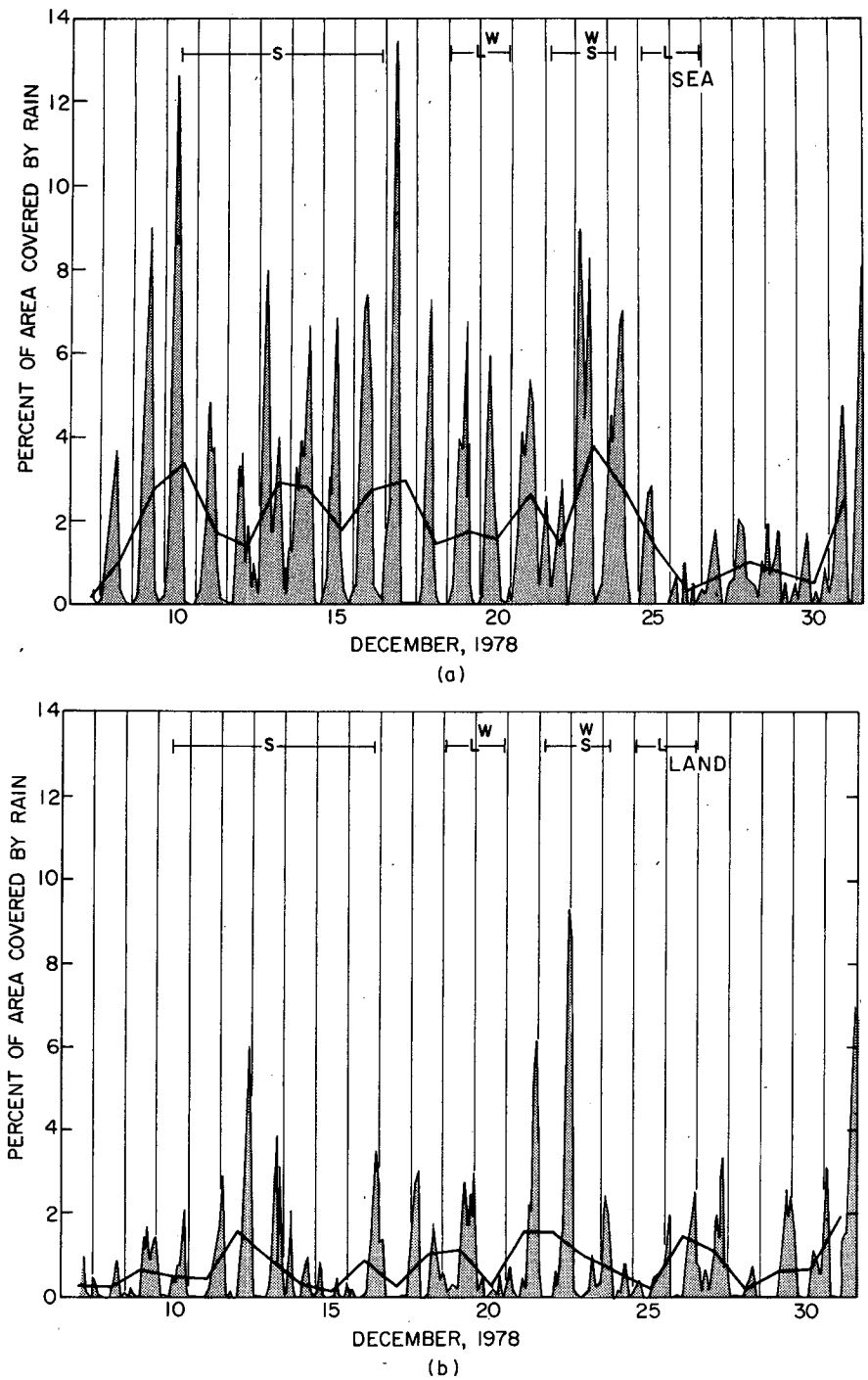

FIG. 10. Time-series of percent of area covered by precipitation, observed over land and sea by the MIT radar at Bintulu. Curves with shading connect unfiltered observations at 1 h intervals. Superimposed heavy curves connect sequential 24 h means. S, W and L denote periods of surges, waves and lulls in the synoptic-scale winds. Tick marks are at 0000 LST.

marized by the sequences of horizontal echo patterns in Fig. 11. All four precipitation systems could be traced to an origin as a group of convective cells that appeared between 2200 and 0200 LST, the typical time that the offshore features began to develop (Figs. 4b and 4c). The 10 December and 16 December features formed just offshore (Figs. 11a and 11d) in a rather typical fashion. The cells

on 18 December, somewhat anomalously, formed just inland (Fig. 11g). The formation of the 23 December features was almost overshadowed by the presence of a major mesoscale disturbance inland. This latter disturbance, which was producing heavy rain over Bintulu at 0000 (Fig. 11j), was unusual and unrelated to the diurnal cycle of convection. Despite the presence of the unusual inland mesoscale disturbance, the usual nocturnal development offshore could be seen beginning along the coast northeast of Bintulu at 0000.

After 0200, the convective cells in each case grew and merged while newer cells continued to form until by 0800–0900 a large continuous rain area covered a region of 100–200 km in horizontal dimension (Figs. 11b, 11e, 11h, and 11k). Except for being somewhat closer to shore than normal, the echo patterns in each case closely resembled the mean for this time of day (cf. Fig. 4d). As will be shown below, the continuous rain area present at 0800–0900 was composed in each case of a few convective cells connected by extensive stratiform precipitation of moderate intensity. The satellite-observed cloud cover associated with the large continuous rain area at 0800–0900 was a widespread continuous sheet of cloud with a cirriform top covering an area larger than that of the rain area seen on radar (e.g., Fig. 7 of Johnson and Priegnitz, 1981).

After 0800–0900, the portions of the rain areas nearest shore began to decay such that the centers of gravity of the areas migrated toward the west-northwest. The echoes also had a translational component of motion toward the west-northwest during this time. The decay of the portions of the rain areas closest to shore was evidently associated with the weakening of the land breeze and establishment of the sea breeze, which occurred during this part of the day (Fig. 8). The translation component was the result of advection of the mid-to-upper tropospheric cloud from which the stratiform rain fell by the 200–300 mb level wind (Fig. 1c).

On 16 December, an unusual new line of convective cells formed and extended out of the decaying nocturnally generated echo, which was centered about 240 km northwest of Bintulu at 1107 (Fig. 11f). The origin of this convective line, which was investigated later in the day by a WMONEX research aircraft flight (Houze *et al.*, 1981) is not clear, but its formation may have been favored by the disturbed conditions associated with the surge and wave activity affecting the area at this time (cf. Figs. 9 and 10).

The vertical structure of the offshore precipitation area around 0800, when it was at its peak development, is illustrated in Figs. 12–15 for each of the example cases. In each figure, part (a) is a detailed horizontal map of the radar reflectivity pattern at the 5 km level which corresponds approximately to the melting level. Parts (b)–(d) of Figs. 12–15 are vertical cross sections along the lines indicated in Figs. 12a, 13a, 14a and 15a.

In each case, the large area of precipitation present at 0800 consisted of a few active deep convective cells (e.g., A–I in Figs. 12–15) interconnected by an extensive region of horizontally uniform (or stratiform) precipitation. The horizontal layering of this precipitation was emphasized by the pronounced radar bright band present near 5 km everywhere between active cells in the vertical cross sections of Figs. 12–15. The presence of the extensive bright band, produced by the melting of snow that was drifting slowly downward, indicates an absence of strong convective updraft and downdraft cells over broad areas. Weaker, widespread vertical air motion must have predominated in these regions. These regions of horizontally uniform precipitation and apparently weak uniform vertical air motions occupied most of the area covered by echo. The stratiform precipitation typically extended over horizontal distances of 100 km and often as much as 200 km (e.g., Figs. 12c, 13c, 14b and 14c, 15c). The extensive areal coverage of the uniform precipitation indicates that, at this stage of the offshore precipitation feature's development, as much or more water (by volume or mass) was falling per unit time in the form of stratiform rain as was falling as convective rain.

10. Conceptual model of the offshore cloud system

Over the equatorial Pacific and Atlantic Oceans, "cloud clusters" are identified in satellite data by their cirrus canopies, which have a horizontal dimension of a few hundred to a thousand kilometers (Frank, 1970; Martin and Suomi, 1972). Similar clusters are observed over equatorial South America (Betts *et al.*, 1976) and Africa (Aspliden *et al.*, 1976; Payne and McGarry, 1977; Fortune, 1980). Within the region covered by one cirrus canopy are usually one or more mesoscale regions of rainfall (Leary and Houze, 1979a). The cloud system that forms diurnally off the northern coast of Borneo behaves as a cloud cluster that contains one such mesoscale rainfall area. A conceptual model of the development and decay of the Borneo cluster is shown in Fig. 16.

The cloud system begins as a group of isolated cells when at about midnight the land breeze begins to converge with the low-level monsoon flow just offshore (Fig. 16a). The precipitation evolves into a continuous mesoscale rain area consisting of a combination of deep cells and stratiform rain falling from mid-to-upper level anvil cloud (Fig. 16b). When the sea breeze begins at about noon, the low-

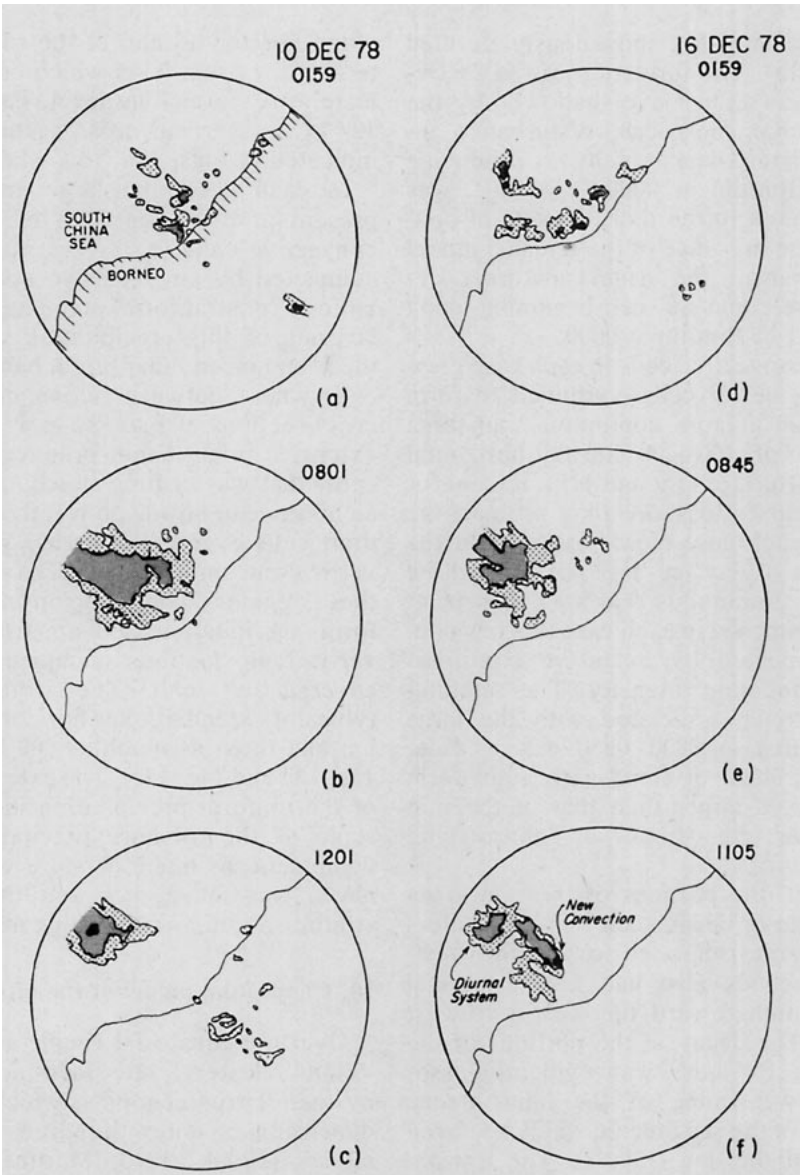

FIG. 11. Low-level radar echo (i.e., precipitation) patterns showing the development of four examples of the mesoscale system generated diurnally off the Borneo coast during the winter monsoon. Intensity thresholds for the three levels of shading are 15, 30 and 45 dBZ. Times indicated are LST.

level convergence and formation of cells ceases and the stratiform precipitation and anvil cloud slowly die out, though the upper level cloud continues to expand horizontally (Fig. 16c).

This life cycle is essentially similar to the life cycles of the individual mesoscale precipitation areas within the cluster studied by Leary and Houze (1979a). They proposed that a mesoscale precipitation feature in a cluster begins in a region of mesoscale convergence. In the Borneo case, the mesoscale convergence is provided once a day by the diurnal wind cycle (Fig. 16a). The mesoscale rain areas described by Leary and Houze matured by a systematic weakening of older convective cells, which merged to form a region of stratiform precipitation, while newer cells continued to form. In Leary and Houze's mesoscale rain areas, the new cells formed systematically at a leading edge, where the low-level convergence was concentrated in a line, and the stratiform region developed systematically to the rear of the line of active cells. In the cloud system off Borneo, the mesoscale convergence apparently does not take place in a line, and new cells form anywhere that low-level convergence becomes concentrated; for example, where the monsoon flow and land breeze converge

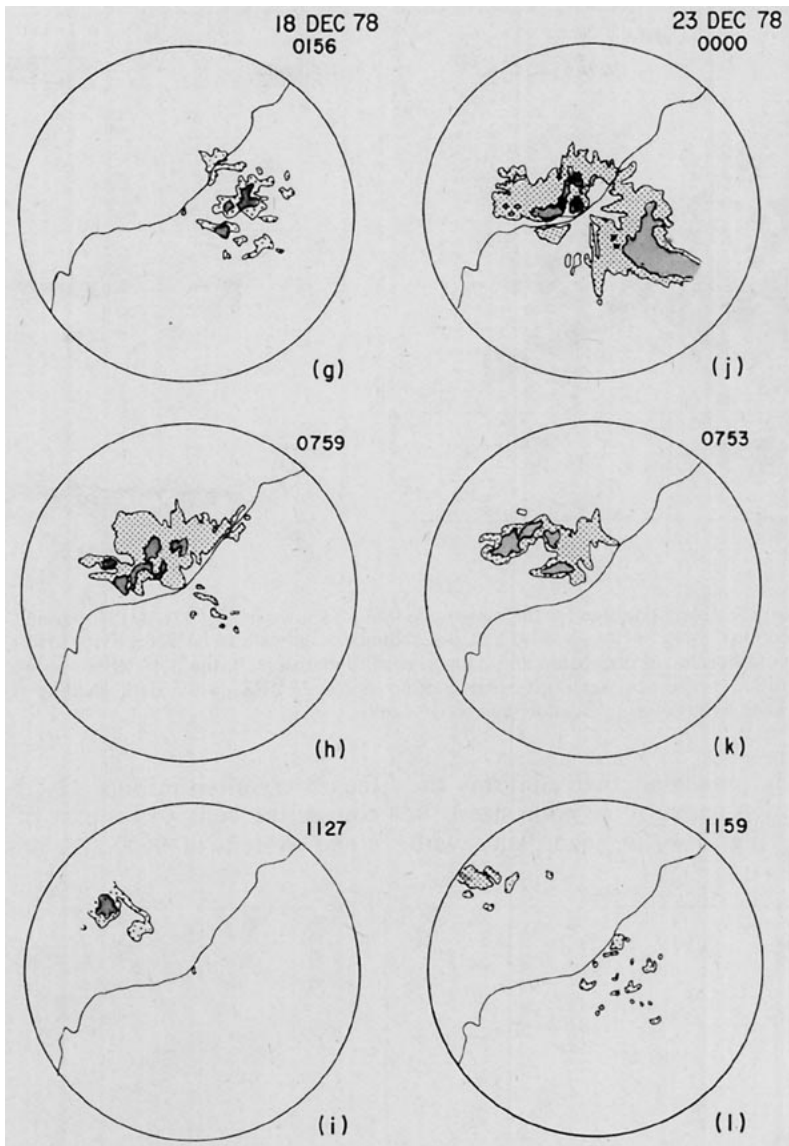

FIG. 11. (*Continued*).

or where downdrafts interact. Consequently, new cells may form on either side of the rain area or within it. Despite this more random pattern of new cell formation, the mesoscale rain area off Borneo resembles those in the cluster studied by Leary and Houze, in growing larger until it consists in its mature stage of several actively growing convective cells interconnected by one large region of stratiform precipitation. In the case of the cloud system off Borneo, this stage is reached at about 0800 LST (Fig. 16b). A characteristic of the Borneo cloud system at this stage is that the upper level cloud canopy, which defines the cluster from a satellite perspective, has spread over a wide area, and it is from this extensive upper tropospheric cloud that the stratiform precipitation falls. In cloud clusters observed elsewhere in the world, the base of this upper "anvil" cloud usually is near the 0°C level. Below this level, melting and evaporation of the falling stratiform precipitation cools the air and drives a gentle mesoscale downdraft ($\sim$10 cm s^{-1} in intensity) (Zipser, 1969, 1977; Brown, 1974, 1979; Houze, 1977; Leary and Houze, 1979b, 1980; Leary, 1980). Although no direct observational evidence of its existence has been previously published, there is reason to believe that a mesoscale updraft, similar in magnitude and extent to the mesoscale downdraft exists within the anvil cloud itself (Houze and Betts, 1981). These kinematic features are incorporated schematically into Figs. 16b and 16c. In the companion paper by Johnson and Priegnitz (1981), evidence from the WMONEX Soviet ship

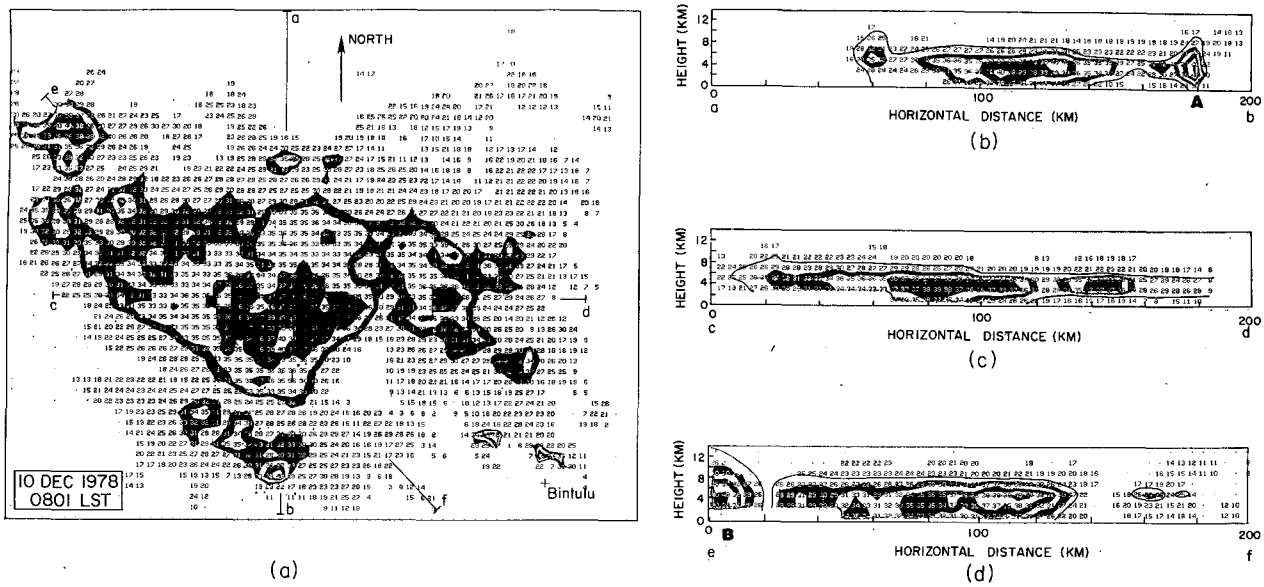

FIG. 12. Detailed radar reflectively patterns for the mesoscale system shown in Fig. 11b. (a) Horizontal pattern at the 5 km level; (b)–(d) vertical cross sections along lines a–b, c–d and e–f. Numbers indicate radar reflectivity (dBZ) averaged over Cartesian grid spaces 4 km × 4 km in horizontal dimension and 2 km vertical dimension. In the horizontal section, dark shading is used for 30–33 dBZ and 36–39 dBZ. In vertical sections, solid contour is for 25 dBZ, while dark shading is used for 28–30, 33–36, and 39–42 dBZ. Upper case letters A and B denote convective cells.

sounding network is presented that confirms the mesoscale air motion pattern hypothesized in Figs. 16b and 16c. Fig. 16b, in accordance with the observations in Figs. 12–15, shows a few active convective cells to be part of the mature Borneo cloud system at 0800. At this time, winds were

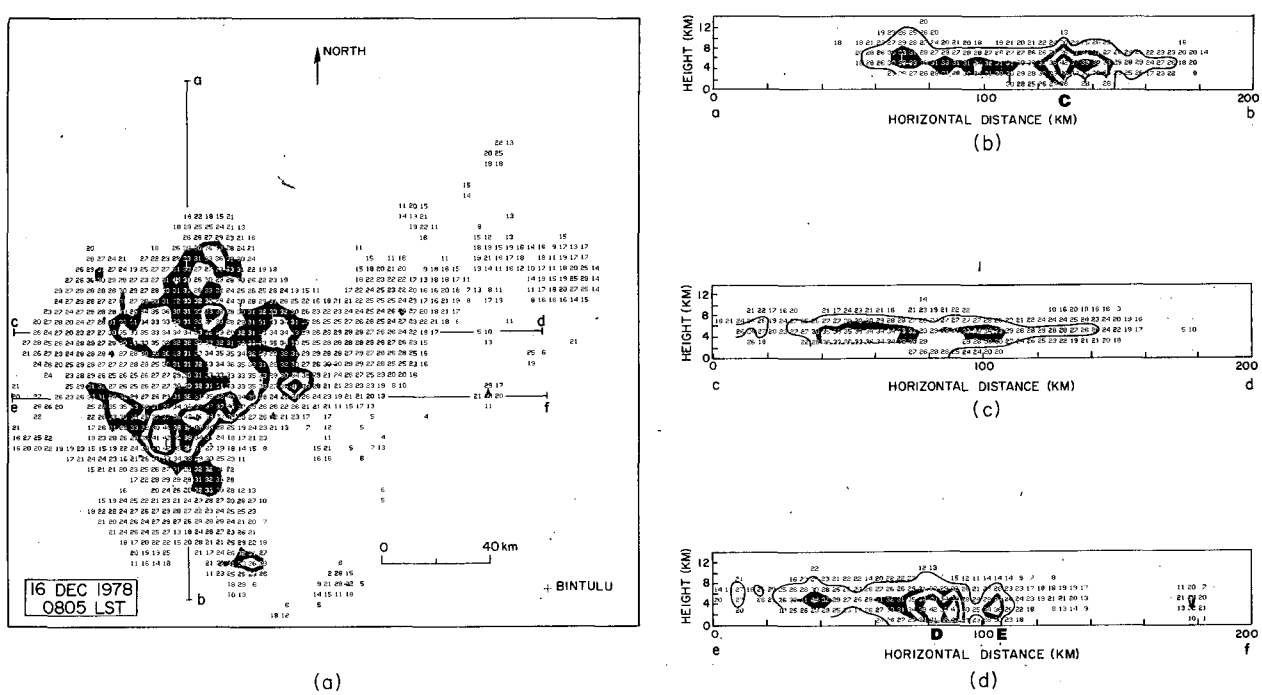

FIG. 13. Detailed radar reflectively patterns for the mesoscale system shown in Fig. 11e. (a) Horizontal pattern at the 5 km level; (b)–(d) vertical cross sections along lines a–b, c–d and e–f. Numbers indicate radar reflectivity (dBZ) averaged over Cartesian grid spaces 4 km × 4 km in horizontal dimension and 2 km vertical dimension. Dark shading is used for 30–33, 36–39, and 42–25 dBZ. In vertical sections, the solid contour is for 25 dBZ. Upper case letters C, D and E denote convective cells.

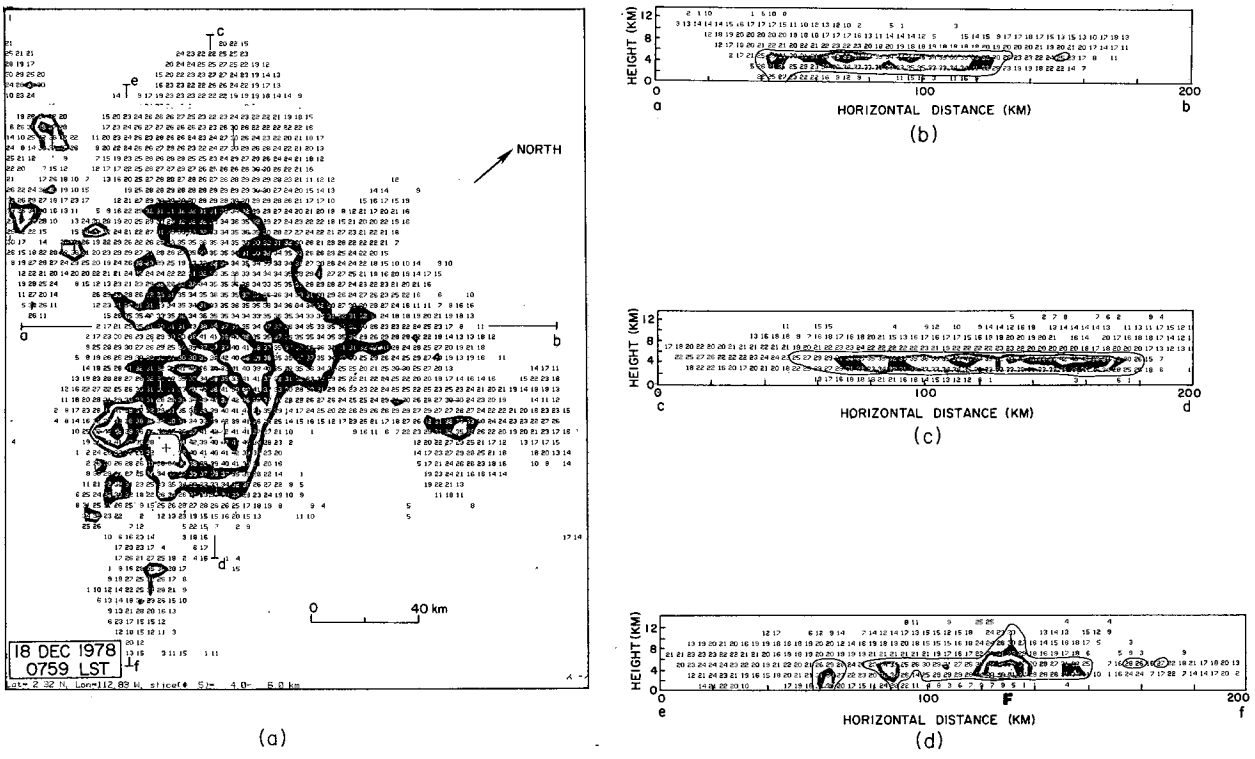

FIG. 14. Detailed radar reflectivity patterns for the mesoscale system shown in Fig. 11h. (a) Horizontal pattern at the 5 km level; (b)–(d) vertical cross sections along lines a–b, c–d and e–f. Numbers indicate radar reflectively (dBZ) averaged over Cartesian grid spaces of 4 km × 4 km in horizontal dimension and 2 km in vertical dimension. Dark shading is used for 30–33, 36–39 and 42–45 dBZ. In vertical cross sections, the solid contour is for 25 dBZ. Upper case F denotes a convective cell.

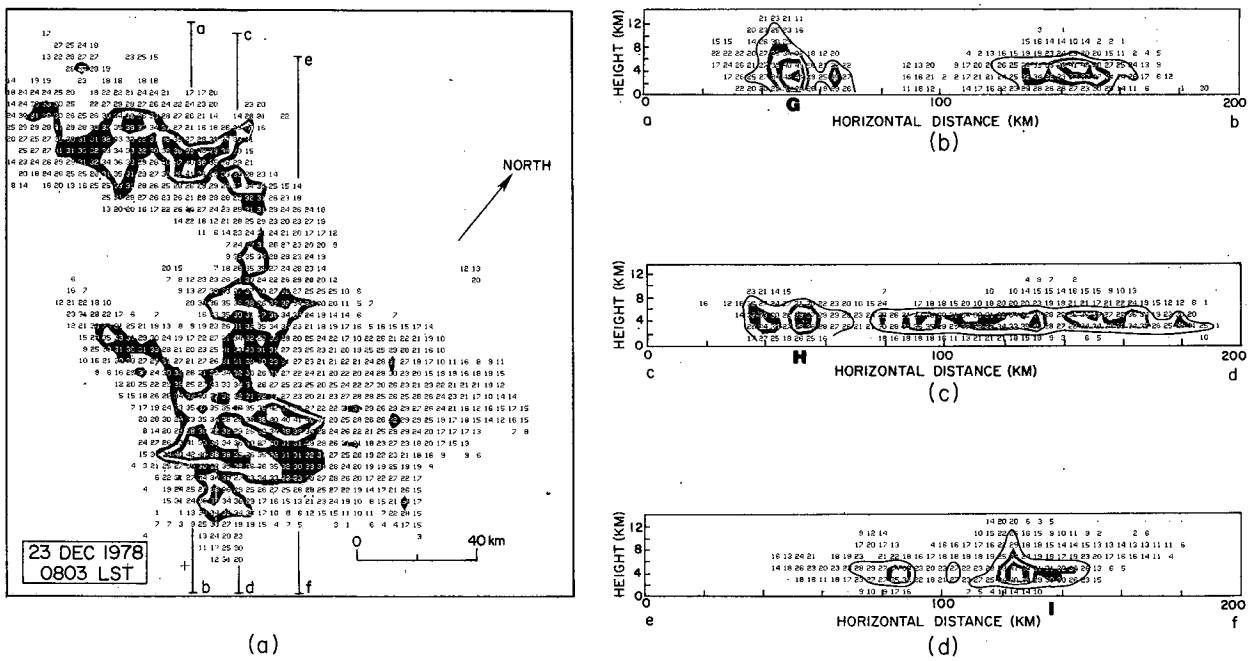

FIG. 15. Detailed radar reflectivity patterns for the mesoscale system shown in Fig. 11k. (a) Horizontal pattern at the 5 km level; (b)–(d) vertical cross sections along lines a–b, c–d and e–f. Numbers indicate radar reflectivity (dBZ) averaged over Cartesian grid spaces of 4 km × 4 km in horizontal dimension and 2 km in vertical dimension. Dark shading is used for 30–33, 36–39 and 42–45 dBZ. In vertical cross sections the solid contour is for 25 dBZ. Upper case G, H and I denote convective cells.

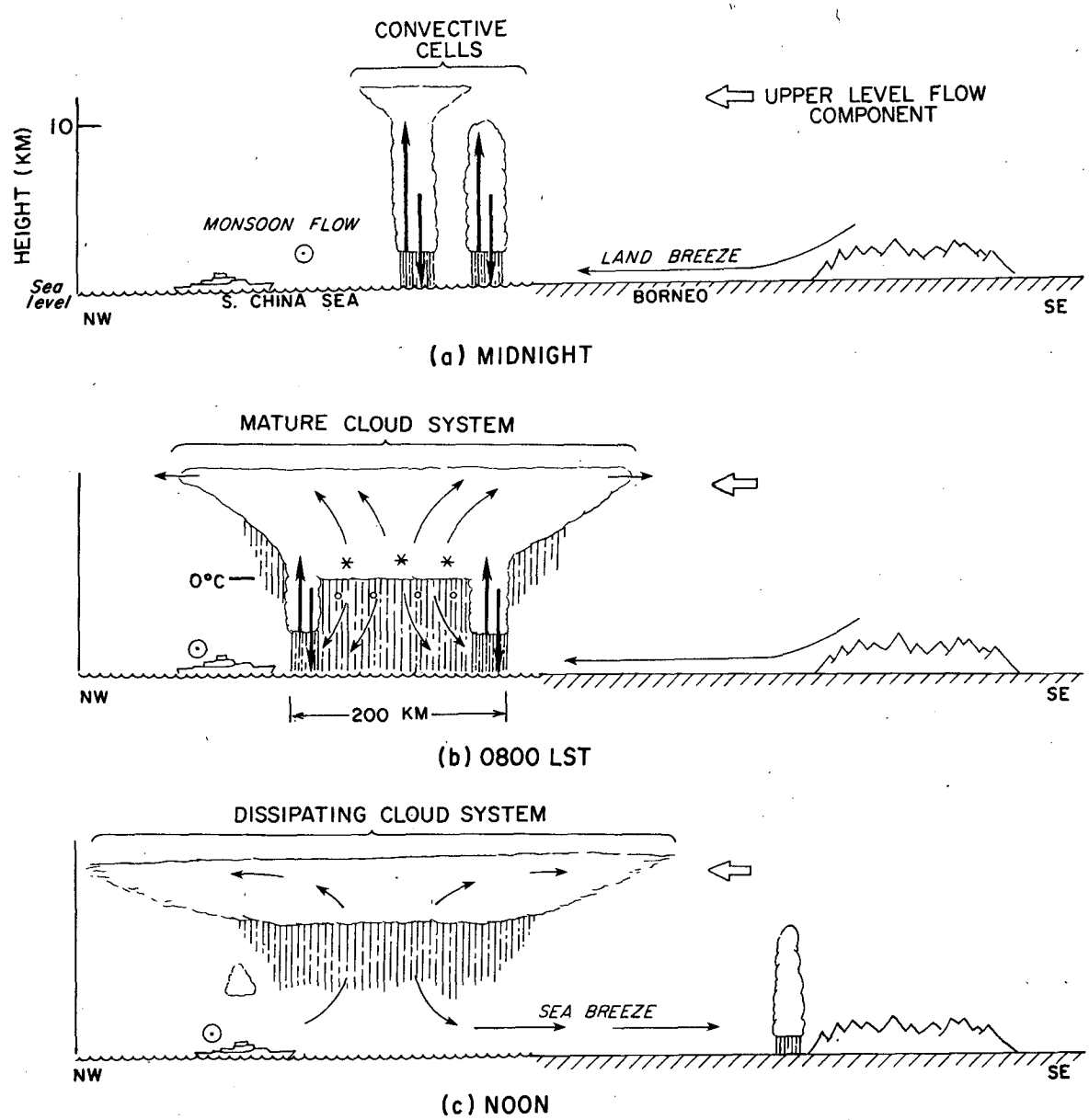

FIG. 16. Schematic of the development of diurnally generated mesoscale precipitation feature off the coast of Borneo. Various arrows indicate airflow. Circumscribed dot indicates northeasterly monsoon flow out of page. Wide open arrow indicates the component of the typical east-southeasterly upper level flow in the plane of the cross section. Heavy vertical arrows in (a) and (b) indicate cumulus-scale updrafts and downdrafts. Thin arrows in (b) and (c) show a mesoscale updraft developing in a mid-to-upper level stratiform cloud with a mesoscale downdraft in the rain below the middle-level base of the stratiform cloud. Asterisks and small circles indicate ice above the 0°C level melting to form raindrops just below this level.

usually still in an offshore direction (Fig. 8) and mesoscale convergence could have occurred on the southeast side of the rain area, where downdraft outflow converged with the offshore land breeze, and on its northwest side, where the downdraft outflow met the monsoon flow. By noon (Fig. 16c), typically, heating over Borneo had produced a sea breeze, and the opportunity for air from the land to converge with either the downdraft or monsoonal air over the sea was thereby cut off. New cell formation could have continued on the northwest side of the cloud system where the monsoonal flow was still meeting downdraft air. However, as the anvil cloud and its associated precipitation were carried farther out to sea by the upper level flow, the cloud system probably encountered an environment of drier, generally subsiding monsoon air in the mid-troposphere, and any new convective

clouds forming in response to the low-level convergence would consequently have been small and suppressed. Eventually, the upper level clouds ceased precipitating and usually by late evening had nearly evaporated.

11. Conclusions

Detailed sequences of radar and satellite observations obtained during WMONEX show that the winter monsoon convection over Borneo and the adjacent southern South China Sea was strongly influenced by the oscillation of the low-level land-sea breeze associated with the daily heating cycle over the island. The general level of convective activity over the sea just north of Borneo was increased when the region was affected by synoptic-scale surges in the low-level northeasterlies over the South China Sea and westward-propagating near-equatorial disturbances that moved into the region. Lulls in the northeasterlies were associated with decreased convective activity over the sea. The diurnal variation in clouds and precipitation remained well defined throughout these periods in which the general level of convective activity was enhanced or suppressed by larger scale events. The diurnal cycle and general level of convective activity over land (at least in the region sampled in this study) were not much affected by synoptic-scale events.

Detailed observations of the offshore convection showed that it typically took the form of a sequence of cloud clusters generated diurnally by the convergence of the land breeze from Borneo with the low-level northeasterly monsoon flow just off the northern coast of the island. Near midnight, the beginning of this convergence tended to trigger a group of convective cells, which then followed a pattern of development slimilar to cloud clusters in other parts of the tropics. Older cells merged to form a continuous region of precipitation falling from an expanding stratiform anvil cloud in the mid-to-upper troposphere. New cells continued to form as long as the land breeze continued. By 0800 LST, the rain area of the cloud cluster resembled the rain areas of other tropical clusters. At this stage, it consisted partly of new active deep convective cells but primarily of stratiform precipitation falling from the anvil cloud. With the cessation of the land breeze and onset of the sea breeze, the generation of new convective cells shifted from the sea to land and the remains of the offshore cloud system drifted out to sea where it slowly dissipated as it encountered an increasingly dry and subsiding air mass.

The structural similarity of the diurnally generated offshore cloud clusters north of Borneo to cloud clusters in other parts of the tropics indicates that their air motions might also be similar. In particular, the presence of widespread anvil precipitation suggests the presence of mesoscale as well as cumulus-scale updrafts and downdrafts in these cloud systems. The companion paper by Johnson and Priegnitz (1981) confirms the existence of the mesoscale drafts. These mesoscale motions can contribute to the vertical transports of mass, heat and other quantities (Johnson, 1980; Leary and Houze, 1980). The extensive stratiform clouds and precipitation in the mid-to-upper troposphere, moreover, can strongly affect the vertical transfer of radiation (Webster and Stephens, 1980). In view of these observations and conclusions, stratiform clouds and precipitation near Borneo and their associated mesoscale circulations should be considered in future studies of winter monsoon dynamics.

Acknowledgments. This research was supported by the Global Atmospheric Research Program, Division of Atmospheric Sciences, National Science Foundation under Grants ATM 78-00232 and ATM80-17327. This paper is Contribution No. 576, Department of Atmospheric Sciences, University of Washington.

REFERENCES

Aspliden, C. I., Y. Tourre and J. C. Sabine, 1976: Some climatological aspects of West African disturbance lines during GATE. *Mon. Wea. Rev.*, **104,** 1029–1035.

Atkinson, G. D., and J. C. Sadler, 1970: Mean-cloudiness and gradient level wind charts over the tropics. Tech. Rep. 215, Vol. II, U.S. Air Weather Service, 48 pp., [AD-711 832].

Betts, A. K., R. W. Grover and M. W. Moncrieff, 1976: Structure and motion of tropical squall lines over Venezuela. *Quart. J. Roy. Meteor. Soc.*, **102,** 395–404.

Blackmon, M. L., J. M. Wallace, N.-C. Lau and S. L. Mullen, 1977: An observational study of the Northern Hemisphere wintertime circulation. *J. Atmos. Sci.*, **34,** 1040–1063.

Brown, J. M., 1974: Mesoscale motions induced by cumulus convection: a numerical study. Ph.D. thesis, MIT, 206 pp.

——, 1979: Mesoscale unsaturated downdrafts driven by rainfall evaporation: A numerical study. *J. Atmos. Sci.*, **36,** 313–338.

Chang, C.-P., J. E. Erickson and K. M. Lau, 1979: Northeasterly cold surges and near-equatorial disturbances over the Winter MONEX area during December 1974. *Mon. Wea. Rev.*, **107,** 812–829.

Cheang, B. K., 1977: Synoptic features and structures of some equatorial vortices over the South China Sea in the Malaysian region during the Winter Monsoon, December, 1973. *Pure Appl. Geophys.*, **115,** 1303–1333.

Cobb, R. T., and L. J. M. Coleby, 1966: *Monsoon Lands, Part I: General Introduction, India, Pakistan, Ceylon, Burma*. Advanced Level Geography Series, University Tutorial Press, 303 pp.

Fortune, M., 1980: Properties of African disturbance lines inferred from time-lapse satellite imagery. *Mon. Wea. Rev.*, **108,** 153–168.

Frank, N. L., 1970: Atlantic tropical systems of 1969. *Mon. Wea. Rev.*, **98,** 307–314.

Gray, W. M., and R. W. Jacobson, Jr., 1977: Diurnal variation of oceanic deep cumulus convection. *Mon. Wea. Rev.*, **105,** 1171–1188.

Houze, R. A., Jr., 1977: Structure and dynamics of a tropical squall-line system observed during GATE. *Mon. Wea. Rev.*, **105**, 1540–1567.

——, and A. K. Betts, 1981: Convection in GATE. *Rev. Geophys. Space Phys.*, **19** (in press).

——, S. G. Geotis, F. D. Marks, Jr., D. D. Churchill and P. H. Herzegh, 1981: Comparison of airborne and land-based radar measurements of precipitation during Winter MONEX. *J. Appl. Meteor.*, **20**, 772–783.

Johnson, R. H., 1980: Diagnosis of convective and mesoscale motions during Phase III of GATE. *J. Atmos. Sci.*, **37**, 733–753.

——, and D. L. Priegnitz, 1981: Winter monsoon convection in the vicinity of North Borneo. Part II: Effects on large-scale fields. *Mon. Wea. Rev.*, **109**, 1619–1632.

Krishnamurti, T. N., M. Kanamitsu, W. J. Koss and J. D. Lee, 1973: Tropical east-west circulations during the northern winter. *J. Atmos. Sci.*, **30**, 780–787.

Leary, C. A., 1980: Temperature and humidity profiles in mesoscale unsaturated downdrafts. *J. Atmos. Sci.*, **37**, 784–796.

——, and R. A. Houze, Jr., 1979a: The structure and evolution of convection in a tropical cloud cluster. *J. Atmos. Sci.*, **36**, 437–457.

——, and ——, 1979b: Melting and evaporation of hydrometeors in precipitation from the anvil clouds of deep tropical convection. *J. Atmos. Sci.*, **36**, 669–679.

——, and ——, 1980: The contribution of mesoscale motions to the mass and heat fluxes of an intense tropical convective system. *J. Atmos. Sci.*, **37**, 784–796.

Manabe, S., J. L. Holloway, Jr., and H. M. Stone, 1970: Tropical circulations in a time-integration of a global model of the atmosphere. *J. Atmos. Sci.*, **27**, 580–613.

Martin, D. W., and V. E. Suomi, 1972: A satellite study of cloud clusters over the tropical North Atlantic Ocean. *Bull. Amer. Meteor. Soc.*, **53**, 135–156.

McGarry, M. M., and R. J. Reed, 1978: Diurnal variations in convective activity and precipitation during Phases II and III of GATE. *Mon. Wea. Rev.*, **106**, 101–113.

Murakami, T., and M. S. Unninayar, 1977: Atmospheric circulation during December 1970 through February 1971. *Mon. Wea. Rev.*, **105**, 1024–1038.

Neumann, J., 1951: Land breezes and nocturnal thunderstorms. *J. Meteor.*, **8**, 60–67.

Payne, S. W., and M. M. McGarry, 1977: The relationship of satellite inferred convective activity to easterly waves over west Africa and the adjacent ocean during Phase III of GATE. *Mon. Wea. Rev.*, **105**, 413–420.

Ramage, C. S., 1968: Role of a tropical "maritime continent" in the atmospheric circulation. *Mon. Wea. Rev.*, **96**, 365–370.

——, 1971: *Monsoon Meteorology*. Academic Press, 271 pp.

Short, D. A., and J. M. Wallace, 1980: Satellite-inferred morning-to-evening cloudiness changes. *Mon. Wea. Rev.*, **108**, 1160–1169.

Webster, P. J., 1972: Response of the tropical atmosphere to local, steady, forcing. *Mon. Wea. Rev.*, **100**, 518–541.

——, and G. L. Stephens, 1980: Tropical upper-tropospheric extended clouds: Inferences from Winter MONEX. *J. Atmos. Sci.*, **37**, 1521–1541.

Zipser, E. J., 1969: The role of organized unsaturated convective downdrafts in the structure and decay of an equatorial disturbance. *J. Appl. Meteor.*, **8**, 799–815.

——, 1977: Mesoscale and convective-scale downdrafts as distinct components of squall-line circulation. *Mon. Wea. Rev.*, **105**, 1568–1589.